# The Reflection of Atomic Beams from Sodium Chloride Crystals

By R. M. ZABEL
*Physical Laboratory, State University of Iowa*

(Received August 26, 1932)

The wave nature of helium, neon, and argon has been investigated by the reflection of beams of these gases from a freshly cleaved surface of sodium chloride. Evidence of diffraction was obtained in all cases, it being most pronounced in helium and least in argon. Both natural and laboratory grown crystals were used. The laboratory grown crystals were cleaved in moist air, dry air, and dry hydrogen. Laboratory grown crystals cleaved in dry air or dry hydrogen reflected a greater percentage of the incident molecules in the specular and diffracted beams than natural crystals or laboratory grown crystals exposed to moist air. The diffraction pattern obtained from crystals which had not been exposed to water vapor was produced by the spacing between rows of sodium and chlorine ions (1.99A). Crystals which had been exposed to water vapor showed evidence of a spacing twice as long as those which had not been exposed.

## INTRODUCTION

IT HAS been established for some time that quantum mechanics correctly describes the motion of free atoms and molecules. The recent experiments of Esterman and Stern[1,2] with hydrogen molecules and helium atoms and of Johnson[3] with hydrogen atoms have shown that both atoms and molecules exhibit properties of a wave motion of wave-length $\lambda = h/mv$ when reflected from the surface of a crystal.

The present investigation was undertaken first to study the effect of the treatment of the surface of the sodium chloride crystal upon the reflection obtained and second to study the reflection of neon and argon from sodium chloride.

## APPARATUS

The beam system used in this experiment is similar to one previously described[4] but it has been enlarged to permit greater pumping speed. Fig. 1 shows the arrangement of the crystal and detector in the beam system and the important dimensions. A special vertical slit $1 \times 0.5$ mm placed in the experimental chamber near the crystal greatly reduces the size of the penumbra of the beam.

The pressures in the various parts of the beam system are of the same order of magnitude as those previously described[4] except that the pressure behind the first opening is necessarily somewhat higher because a channel is used where a hole in a thin wall had been used in the previous system. The pressure in this portion of the apparatus is normally about 6 mm of mercury for helium, 2.5 mm for argon and 1.5 mm for neon.

[1] Esterman and Stern, Zeits. f. Physik **61**, 95 (1930).
[2] Esterman, Frisch, and Stern, Zeits. f. Physik **73**, 348 (1931).
[3] T. H. Johnson, Phys. Rev. **37**, 847 (1931).
[4] A. Ellett and R. M. Zabel, Phys. Rev. **37**, 1112 (1931).

Fig. 2 shows two views of the apparatus which controls the position of the detector and crystal. The detector nozzle rotates about the crystal on a horizontal axis $A$ perpendicular to the direction of the beam. Its position is indicated by the scale $B$. The crystal holder may be rotated about the beam as an axis. The method of producing this rotation is evident by a comparison of the two views since the one is taken with a considerably different setting than the other. Rotation of the crystal is also possible about the axis $CD$ perpendicular to the beam so that the normal to the crystal may be pointed in any desired direction. The position of the crystal is indicated by the scales $E$ and $F$. The combined motion of the crystal and gauge makes possible the complete study (except for the region between the incident beam and the

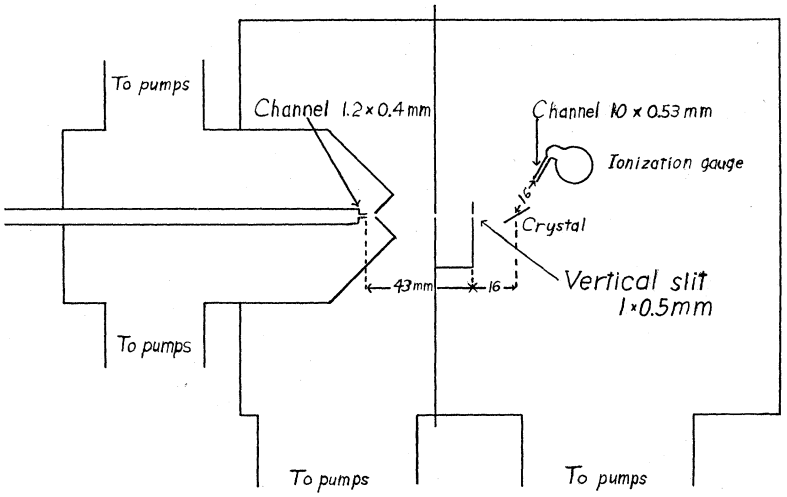


Fig. 1. The beam system.

crystal) of the reflection from a crystal with any desired angle of incidence. The crystal holder may also be lowered to permit measurement of the intensity of the incident beam. The four controls described above are operated magnetically by short bars on the end of four concentric tubes $G$.

An ionization gauge is used to detect the beam. A diagrammatic sketch of the gauge and its connections is shown in Fig. 3. In spite of the small size of the gauge, the plate is highly insulated by supporting it entirely from its tungsten lead. The Pyrex wall of the gauge is protected from evaporation of the filament by the plate itself. The grid is composed of the least number of turns which permit the gauge to be operated under normal conditions free from Barkhausen oscillations. The gauge is normally operated at 10 m.a. electron current as this value has been found experimentally to give the best balance between sensitivity and stability of the gauge. The sensitivity of the gauge is of the order of $5\times10^{-10}$ mm of mercury per mm galvanometer deflection. The current due to the residual pressure in the experimental chamber is balanced out of the galvanometer by the simple circuit shown. The current under high-vacuum conditions is approximately $10^{-7}$ amperes

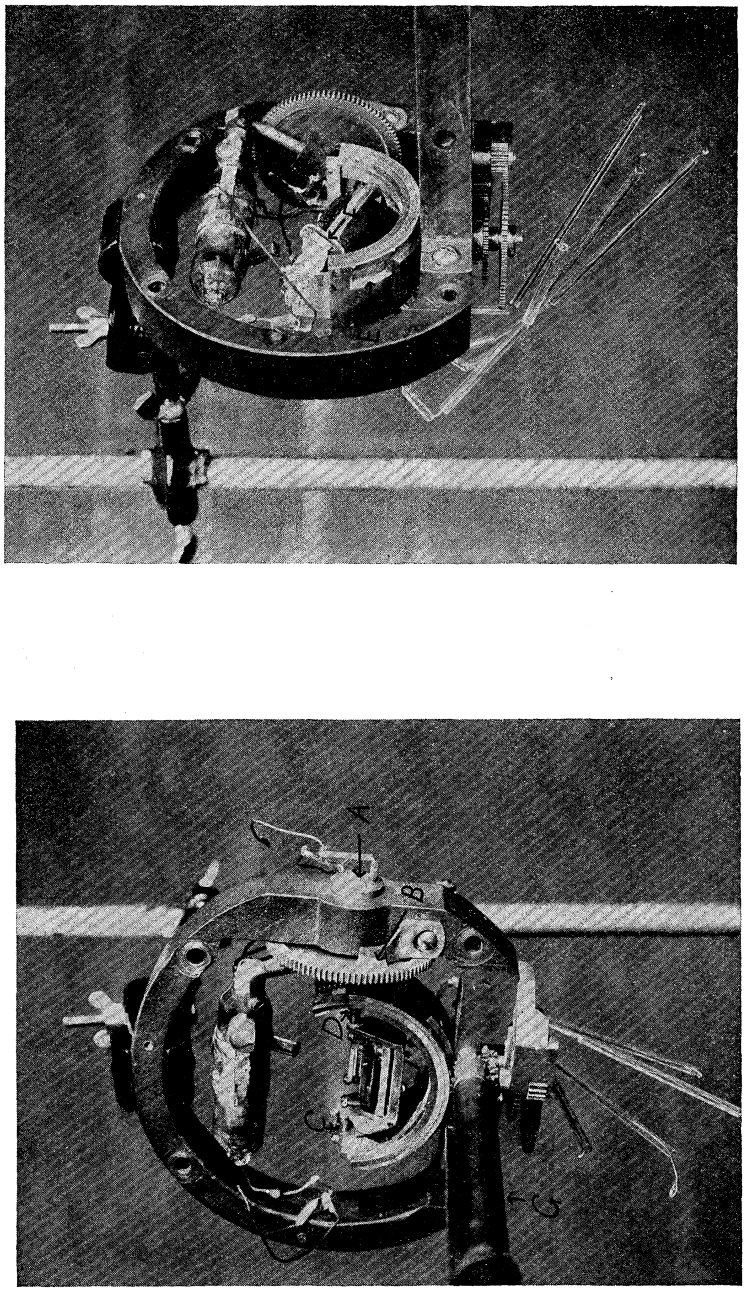


Fig. 2. Two views of detector and crystal rotating mechanism.

(corresponding to a pressure of the order of $10^{-6}$ mm of mercury) and is increased from 20 to 50 percent when the beam is in operation. The percentage increase in current due to the beam depends, of course, upon the kind of gas forming the beam and upon the beam intensity.

Since no attempt is made to compensate for general pressure changes in the experimental chamber one might expect considerable difficulty in maintaining a steady zero of the galvanometer. Such is not the case, however. The zero is checked before and after each reading and the two values normally agree within a few percent of the reading. The use of a compensating gauge might make the use of a more sensitive current measuring instrument feasible.

The gas used in forming the beam is exhausted by the various pumps operating directly on the beam system into a common chamber which is in turn pumped out by a set of special diffusion pumps capable of pumping

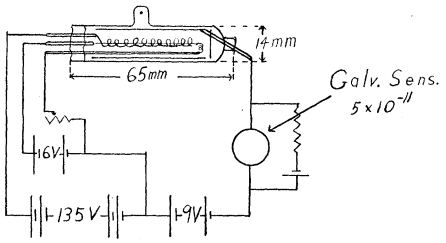


Fig. 3. The ionization gauge.

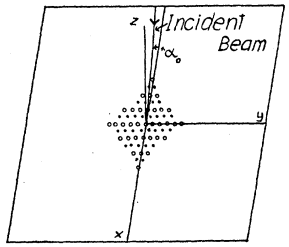


Fig. 4. Relative position of crystal and incident beam.

rapidly against high pressure. This set of pumps exhausts into another chamber which is connected to the first slit of the beam system so that the gas used in forming the beam may be continually circulated. The gas is purified as it circulates by passing it through a liquid air trap and a hot cathode misch metal arc. A hot cathode is used in the arc because the pressure is frequently too low for the satisfactory operation of an ordinary arc.

The crystals used in these reflection experiments were grown in this laboratory by Dr. R. Hancox and the author by the method recently developed by Strong.[5]

The treatment of the crystal surface after cleaving seems to have a very marked influence on the resulting reflection, hence it is discussed in some detail. The normal procedure in making a run is to evacuate the system for several days, fill it with dry hydrogen or dry air, cleave the crystal in an atmosphere of dry hydrogen, dry air, or moist air as desired and place it in the apparatus without exposure to any gas except that in which it was cleaved. When the crystal is cleaved in a dry atmosphere, the hydrogen or air used to fill the apparatus and the chamber in which the crystal is cleaved is passed through a long tube filled with $P_2O_5$ in order to dry it thoroughly. A continuous stream of this dry hydrogen or air flows through the cleaving chamber in order to carry away any moisture which might accumulate. The

[5] John Strong, Phys. Rev. **36**, 1663 (1930).

cleaving process is carried on in a large tin box with two holes in the sides to permit entrance of the hands and a third hole through which to place the crystal into the apparatus. These holes were made gas tight by the use of rubber sheeting. Perspiration from the operator's hands was avoided by covering them with rubber gloves during the cleaving process. After cleaving the crystal its thickness is measured, a metal sheet is chosen to place under the crystal to give the surface the proper height and the crystal and metal sheet are mounted on the crystal holder under molybdenum springs. The crystal holder is then placed in a beveled groove (see Fig. 2) in the apparatus through a ground joint by the aid of a long tweezer. The ground joint is sealed by glycolphthalic anhydride resin.[6] An electric heater warms the joint so that it may be sealed merely by placing the parts together. Evacuation is started about thirty seconds after the crystal is cleaved and is complete in about fifteen minutes. The crystal is immediately heated to 350°C where it is maintained for several hours after which it is cooled to 100° or 150°C and is maintained at that temperature while readings are taken.

## Diffraction Patterns

Assuming that the ions in the surface layer of the crystal act as scattering points of a grating, the resulting diffraction pattern should be governed by the equations

$$\cos\alpha - \cos\alpha_0 = h_1\lambda/d \tag{1}$$

$$\cos\beta - \cos\beta_0 = h_2\lambda/d \tag{2}$$

where $\alpha$ and $\beta$ are the angles measured from the principal axes (rows of like ions) in the crystal surface.

Fig. 4 shows the normal position of the crystal with respect to the beam, the plane of incidence being parallel and perpendicular to the principal axes of the crystal. Eq. (2) then reduces to

$$\cos\beta = h_2\lambda/d. \tag{3}$$

The spectra investigated are given by (1) and (3) when $h_1 = \pm 1$ and $h_2 = 0$ and when $h_1 = 0$ and $h_2 = \pm 1$. The first type is found in the plane of incidence. The second is found by moving the detector along the intersection of the cone making a constant angle $\alpha_0$ about the $x$ axis (Fig. 4) and a cone making a variable angle $\beta$ about the $y$ axis or by moving the crystal and detector to obtain the same resultant motion.

In order to determine the position of the detector so that it will be on the diffraction cone and the relation between the angle $\beta$ of Eq. (3) and the angle $\theta$ (taken from the apparatus) through which the crystal is rotated about the beam, consider Fig. 5. The axes $x$ and $y$ are parallel to the principal axes in the surface of the crystal and $z$ is the crystal normal. The $x'$ and $x$ axes coincide, the $y'$ axis coincides with the incident beam and the $z'$ axis completes the primed system. With the crystal in this position the specular beam

[6] Sager and Kennedy, Physics **1**, 352 (1931).

($h_1 = h_2 = 0$) will be observed when the detector is raised $2\alpha_0$ above the negative $y'$ axis. As the crystal is rotated through an angle $\theta$ about the incident beam (part I, Fig. 5) the $x$, $y$ and $z'$ axes take the positions denoted by $x''$, $y''$ and $z''$. The negative $y''$ axis will not be in the $y'z'$ plane defined by

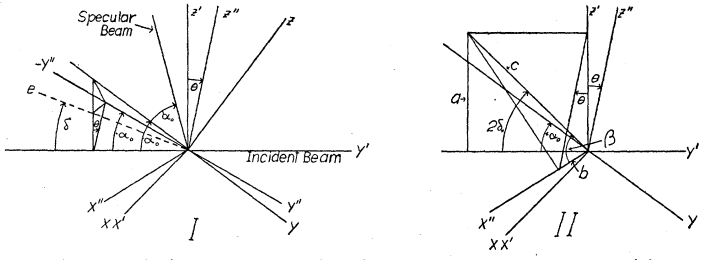


Fig. 5. Relations of angle taken from apparatus to $\beta$ of Eq. (3).

the incident beam and the detector. Its projection in this plane is the line indicated as $e$. The angle which $e$ makes with the negative $y'$ axis is given by the equation

$$\delta = \tan^{-1}(\tan \alpha_0 \cos \theta). \tag{4}$$

Twice $\delta$ is then the angle, computed for any value of $\theta$, above the negative $y'$ axis at which the detector must be placed in order to be on the cone making an angle $\alpha_0$ with the negative $y''$ axis. A relation between $\beta$ and $\theta$ may be derived from part II of Fig. 5 as follows:

$$\cos \beta = b/c, \quad \sin \theta = b/a, \quad \sin 2\delta = a/c.$$

From the above equations $\cos \beta = \sin 2\delta \sin \theta$. For convenience the angle $\phi$ will be used hereafter where $\phi = 90 - \beta$. Hence

$$\phi = \sin^{-1}(\sin 2\delta \sin \theta). \tag{5}$$

## Diffraction in Helium

Fig. 6 shows the results obtained in the reflection of helium from three distinct crystal surfaces. The curves have been plotted in terms of the angle $\phi$ where $\phi$ is determined from $\theta$, the rotation of the crystal, by the aid of Eqs. (4) and (5). The crystals were cleaved in an atmosphere of dry hydrogen. There is an increase in the intensity of the specular and diffracted beam as well as a shift of the diffraction maxima to larger angles with each successive crystal. Crystal (1) was exposed to some water vapor as the operator's hands were not covered with rubber gloves during the cleaving of this crystal. Rubber gloves were used in cleaving crystal (2) but it had a poor surface which may account for its poor reflection. Crystal (3) was normal both in appearance and results.

The curves in Fig. 6 were taken with a wider set of slits than those specified in Fig. 1. All the following helium curves were, however, taken with the slits specified in Fig. 1, hence the following curves can not be compared with those in Fig. 6.

Fig. 7 shows the effect of water vapor on the surface of a crystal. Crystal (4) was cleaved in dry hydrogen and curve *a* was obtained. The crystal was then exposed to dry air at a pressure of 10 cm of mercury for several minutes after which curve *b* was obtained. There is no marked difference between the two curves. Crystal (5) was cleaved in dry air and its characteristics are as good as an ordinary crystal cleaved in dry hydrogen. Crystals (6) and (7) were cleaved in wet air (relative humidity 65 percent at 31°C) and both gave a very poor specular beam and diffraction pattern.

Crystal (8) of Fig. 7 was the most satisfactory surface which could be found in a large group of natural crystals as judged by the perfection of its

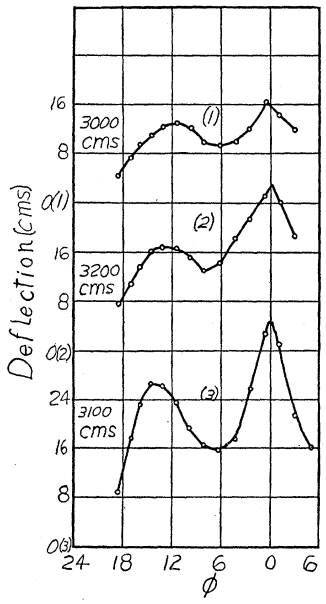


Fig. 6. Reflection of helium from sodium chloride crystals. Notations such as "3000 cm" etc., give the intensity of the incident beam. The numbers in parentheses identify individual crystals.

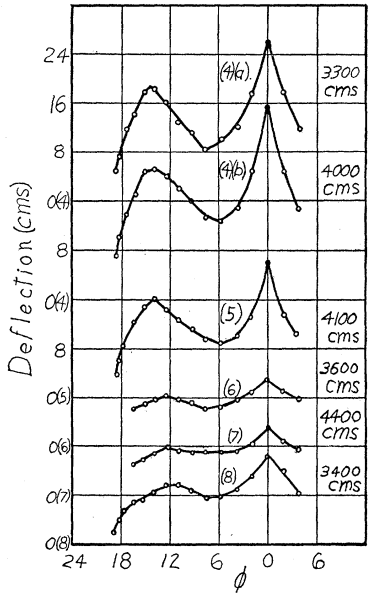


Fig. 7. Effect of water vapor on the "reflecting power" of a crystal surface.

optical reflection. Even this carefully selected crystal was, however, not as satisfactory as the laboratory grown crystals either in its reflection of light waves or particle waves.

The present status of the investigation indicates that there is a close correlation between the reflection of light waves and particle waves from the surface of a crystal. Crystals, either natural or laboratory grown, which give the most perfect optical reflection normally give the most intense specular beams and diffraction patterns.

With the slits specified in Fig. 1 the specular beam, if perfectly reflected, should reduce to zero at three degrees on either side of the peak. There is obviously some diffuseness in the reflection even in the most satisfactory crystals.

Fig. 8 shows the curve obtained by the same relative motion of gauge and crystal as previously described with the crystal turned 45° about its normal (Fig. 4) so that rows of like ions make an angle of 45° with the plane

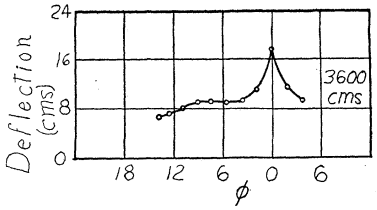


Fig. 8. Spectra from rows containing both sodium and chlorine ions.

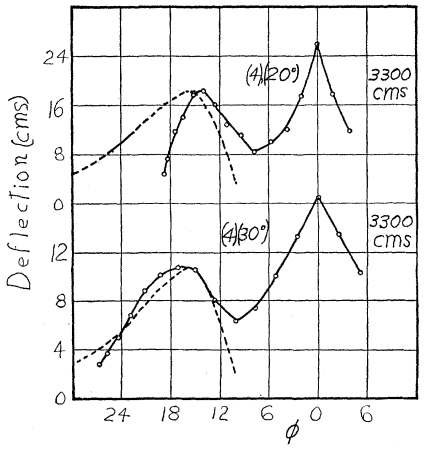


Fig. 9. Comparison of observed wave-length distribution with that calculated from Maxwell's distribution law for angles of incidence of 20 and 30 degrees.

of incidence. Any spectra found in this position would be due to rows which contain sodium and chlorine ions alternately. Obviously spectra do not arise from these rows.

## Wave-Length Distribution

The distribution in velocity of the molecules in the beam is given by Maxwell's law as

$$dI/dv = Ae^{-mv^2/2KT}v^3 \tag{6}$$

if the mean free path behind the first opening of the beam system is long compared to the diameter of the opening and if collisions along the path of the beam are negligible.

Assuming a wave-length $\lambda = h/mv$ associated with each particle of mass $m$ and velocity $v$ Eq. (6) may be written

$$dI/d\lambda = (A'e^{-\lambda_0^2/\lambda^2})/\lambda^5 \tag{7}$$

where

$$\lambda_0 = h/(2mKT)^{1/2}. \tag{8}$$

The diffraction curves are plotted in terms of $\phi$ where

$$\lambda = d \sin \phi. \tag{9}$$

Then

$$d\lambda/d\phi = d \cos \phi. \tag{10}$$

But

$$dI/d\phi = (dI/d\lambda)(d\lambda/d\phi). \tag{11}$$

Substituting from (7), (9) and (10) in (11) one obtains,

$$dI/d\phi = \frac{A'' \exp\left[-\lambda_0^2/d^2 \sin^2\phi\right] \cos\phi}{\sin^5\phi}. \tag{12}$$

Fig. 9 compares the intensity distribution obtained experimentally with that obtained from Eq. (12) for curves taken at angles of incidence of 20° and 30°. It will be noted that at 20° incidence the peak of the diffraction curve is at a smaller angle and the intensity of the diffracted beam falls off more rapidly with large values of $\phi$ than Eq. (12) predicts. This may be expected from geometrical consideration since the diffraction cones are nearing the angle (20°) where they will no longer intersect. In spite of this disadvantage 20° was used as the angle of incidence in almost all the curves because it gave a more intense specular beam and diffraction pattern than 30°.

The experimental and theoretical curves for 30° incidence are in satisfactory agreement in view of the fact that the first opening of the beam system was a channel and that the mean free path behind the channel was short compared to the diameter of the channel. Both the channel and the short mean free path might be expected to distort the wave-length distribution curve.

The grating spacing which produces the observed diffraction pattern may be determined by differentiating the right side of Eq. (12) setting the result equal to zero and solving for $d$ which gives

$$d = \frac{2^{1/2}\lambda_0 \cos\phi_0}{\sin\phi_0} \frac{1}{(\sin^2\phi_0 + 5\cos^2\phi_0)^{1/2}} \tag{13}$$

where $\phi_0$ is the value of $\phi$ at the maximum of the diffraction curve and $\lambda_0$ is 0.888A as determined from Eq. (8) when $T = 300°K$. Table I gives the spacings calculated from Eq. (13) for the various crystals used.

TABLE I. *Spacings computed from the crystals investigated.*

| Crystal number | Note | Spacing in A |
|---|---|---|
| 1 | Exposed to water vapor | 2.80 |
| 2 | | 2.54 |
| 3 | | 2.28 |
| 4 | Before exposure | 2.22 |
| 4 | After exposure | 2.22 |
| 4 | 30° incidence | 1.97 |
| 5 | Cleaved in dry air | 2.28 |
| 6 | Cleaved in wet air | 2.60 |
| 7 | Cleaved in wet air | 2.65 |
| 8 | Natural crystal | 2.80 |

The possible spacings are the distance between rows of like ions (3.98A) or the distance between rows of unlike ions (1.99A). It is evident from the

above table that the shorter spacing or second order spectra from the longer spacing is predominant in these crystals. The fact that the computed spacings at 20° incidence are longer than they should be has been explained in the previous discussion.

Table I shows that crystal surfaces which have been exposed to water vapor have a longer spacing than those which have not. Because of the width of the velocity distribution in the incident beam two peaks arising from spacings of 1.99A and 3.98A would not be resolved. Hence the change in spacing may be interpreted as being due to the fact that a portion of the crystal surface reflects with a spacing of 3.98A after the crystal has been exposed to water vapor. This suggests that on the portion of the surface which acquires the new spacing one molecule of water may be collected by each sodium ion (union with sodium is assumed because of the affinity of sodium for water vapor) in such a way that the water molecules form a grating with a periodicity equal to the distance between rows of sodium ions. On the other hand, one may assume that heating the crystal removes the water vapor and that each molecule of water carries with it some of the ions in the crystal surface in a manner analogous to the removal of the surface when a salt crystal is dissolved in water. The gaps in the crystal surface caused by the removal of these ions would produce the observed increase in periodicity.

The latter hypothesis appears more reasonable than the first in view of the fact a crystal once exposed to water vapor can be heated to 700°C for some time without improving its "reflecting power." In either case the decreased intensity of the specular beam and diffraction pattern could be accounted for by the increased roughness of the surface.

The observed spacing of the natural crystal is also longer than the spacing of laboratory grown crystals. Since the best natural crystals which could be obtained still showed considerable evidence of strain it is possible that the strained condition causes the crystal to cleave imperfectly so that gaps are left in the surface. These gaps might give rise to a variety of spacings all longer than the fundamental spacing observed in the more perfect surfaces so that the tendency would be to shift the curve in the direction of longer spacings. This is in agreement with the results of experiment.

## Diffraction in Neon and Argon

Fig. 10 shows the evidence of diffraction obtained in the case of neon and argon. It will be noted that the crystals used have been used previously with helium. The reflection is much more diffuse and the specular and diffracted beams much less pronounced than in the case of helium. The grating spacing corresponding to the maximum of the neon curve is 2.05A and to the maximum of the argon curve 3A. The diffraction peak of the argon curve has probably been moved toward smaller angles by the rapid decrease in intensity of the diffuse specular beam upon which the diffraction peak is superimposed.

As previously indicated the slits in the apparatus were changed between the study of crystal (3) and crystal (4) so that the argon and neon curves are

not comparable insofar as the relative intensity of the incident and specular beams is concerned.

## Spectra in the Plane of Incidence

Fig. 11 shows the reflection found in the plane of incidence. The angle ($\alpha$ of Eq. (1)) is measured from the plane of the crystal so that the specular beam should occur at 20° in each case. The maximum in the case of neon and argon is shifted by a considerable amount from the expected position of the specular beam. Conclusive evidence of diffraction appears only in the case of helium. There is probably, however, a very interesting relation between the fact that the diffraction peak in the helium curve appears only on

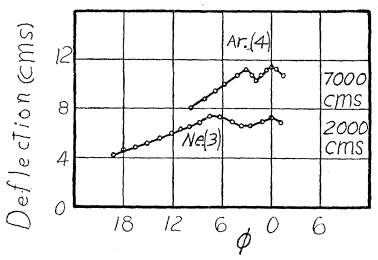


Fig. 10. Diffraction in neon and argon.

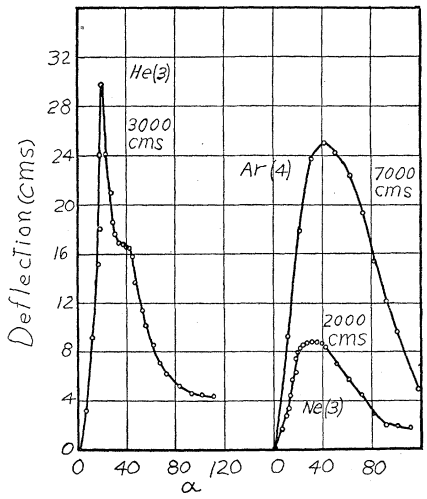


Fig. 11. Curves taken in the plane of incidence.

the large angle side of the specular beam and the fact that the argon and neon curves have a maximum at larger angles than the expected position of the specular beam.

Another point of interest in this connection is the similarity between the argon curve of Fig. 11 and curves obtained in the reflection of mercury from sodium chloride. Zahl and Ellett[7] found in mercury a diffuse directed beam which for small angles of incidence has its maximum closer to the normal than the expected position of the specular beam. The similarity of the argon and mercury curves suggests that they have a common explanation.

In conclusion the writer wishes to express his appreciation to Professor A. Ellett for many helpful suggestions in connection with this investigation.

[7] H. A. Zahl and A. Ellett, Phys. Rev. 38, 977 (1931).

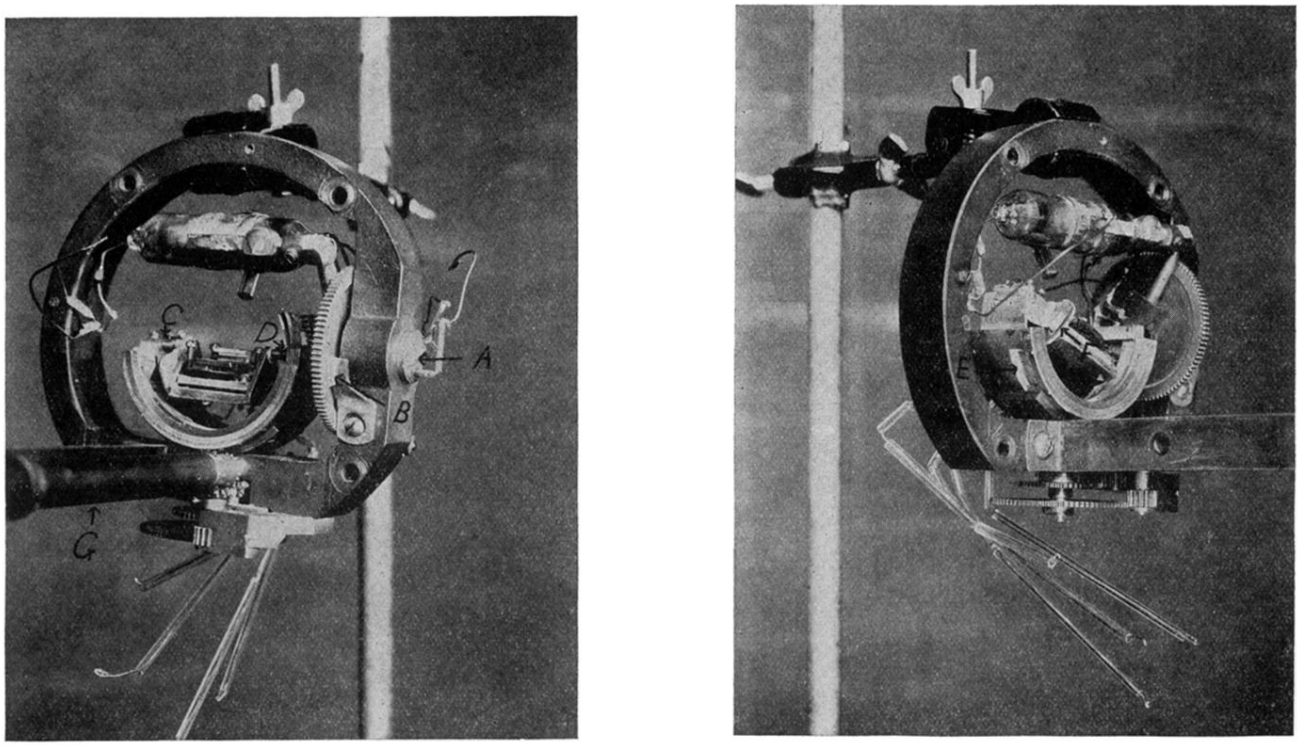


Fig. 2. Two views of detector and crystal rotating mechanism.